Published in final edited form as:

Arch Biochem Biophys. 2001 March 15; 387(2): 243–249. doi:10.1006/abbi.2000.2259.

Calcium- and Magnesium-Dependent Interactions between the C-Terminus of Troponin I and the N-Terminal, Regulatory Domain of Troponin C

Jeanne Digel, **Omoefe Abugo**, **Tomoyoshi Kobayashi**, **Zygmunt Gryczynski**, **Joseph R. Lakowicz**, **John H. Collins**[1]

Medical Biotechnology Center, University of Maryland Biotechnology Institute, 725 West Lombard Street, Baltimore, Maryland 21201; and Department of Biochemistry and Molecular Biology, University of Maryland, School of Medicine, 108 North Greene Street, Baltimore, Maryland 21201

Abstract

The muscle thin filament protein troponin (Tn) regulates contraction of vertebrate striated muscle by conferring Ca^{2+} sensitivity to the interaction of actin and myosin. Troponin C (TnC), the Ca^{2+} binding subunit of Tn contains two homologous domains and four divalent cation binding sites. Two structural sites in the C-terminal domain of TnC bind either Ca^{2+} or Mg^{2+}, and two regulatory sites in the N-terminal domain are specific for Ca^{2+}. Interactions between TnC and the inhibitory Tn subunit troponin I (TnI) are of central importance to the Ca^{2+} regulation of muscle contraction and have been intensively studied. Much remains to be learned, however, due mainly to the lack of a three-dimensional structure for TnI. In particular, the role of amino acid residues near the C-terminus of TnI is not well understood. In this report, we prepared a mutant TnC which contains a single Trp-26 residue in the N-terminal, regulatory domain. We used fluorescence lifetime and quenching measurements to monitor Ca^{2+}- and Mg^{2+}-dependent changes in the environment of Trp-26 in isolated TnC, as well as in binary complexes of TnC with a Trp-free mutant of TnI or a truncated form of this mutant, TnI(1–159), which lacked the C-terminal 22 amino acid residues of TnI. We found that full-length TnI and TnI(1–159) affected Trp-26 similarly when all four binding sites of TnC were occupied by Ca^{2+}. When the regulatory Ca^{2+}-binding sites in the N-terminal domain of TnC were vacant and the structural sites in the C-terminal domain of were occupied by Mg^{2+}, we found significant differences between full-length TnI and TnI(1–159) in their effect on Trp-26. Our results provide the first indication that the C-terminus of TnI may play an important role in the regulation of vertebrate striated muscle through Ca^{2+}-dependent interactions with the regulatory domain of TnC.

Keywords

muscle; regulation; troponin; calcium; fluorescence

Vertebrate striated muscle contraction is regulated by Ca^{2+} and requires the proteins troponin (Tn)[2] and tropomyosin (Tm), located on the actin-containing thin filaments. Tn is

[1]To whom correspondence and reprint requests should be addressed. Fax: (410) 706-7364. collins@umbi.umd.edu.

composed of three subunits: TnC, which binds Ca^{2+}, TnI, which inhibits actomyosin ATPase activity, and TnT, which binds Tm (for recent reviews, see Refs. 1–5). The purpose of this paper is to help delineate functionally important interactions between TnC and TnI.

The crystal structure of vertebrate fast skeletal muscle TnC shows a dumbbell-shaped molecule with two globular domains, each of which contains a pair of Ca^{2+}-binding sites (6–8). The sites in the N-terminal domain are regulatory and Ca^{2+}-specific, while the sites in the C-terminal domain bind both Ca^{2+} and Mg^{2+} and play a structural role. Despite many studies over the past quarter century, much remains to be learned about the three-dimensional structure of TnI and the nature of its extensive and complex interactions with TnC (see Ref. 9 for recent review). TnI binds to TnC in an antiparallel orientation, with the N-terminus of TnC binding the C-terminus of TnI and vice versa (10, 11). The N-terminal region (residues 1–47) and a centrally located inhibitory segment (residues 96–116) of TnI have long been established as sites of interaction with TnC (12). The inhibitory segment, like whole TnI, binds to actin and inhibits actomyosin ATPase activity in the absence of Ca^{2+}. This inhibition can be reversed by TnC in the presence of Ca^{2+} (12). Binding of Ca^{2+} to the regulatory sites of TnC induces localized conformational changes which result in the exposure of a hydrophobic pocket in the N-terminal domain. This pocket interacts with a segment of TnI, residues 115–131, which overlaps the C-terminal part of the TnI inhibitory region (13, 14). Pearlstone *et al.* (15) prepared a spectral probe mutant, F29W, of chicken fast skeletal muscle TnC. In this mutant, Phe-29, which is near one of the regulatory Ca^{2+} binding sites in the N-terminal domain, was replaced by a single Trp residue. The quantum yield of the steady-state fluorescence of F29W increased about threefold in response to Ca^{2+} binding to the N-terminal, regulatory sites of TnC. Binding of Mg^{2+} to the structural sites in the C-terminal domain of TnC did not affect the fluorescence properties of F29W.

Little is known about interactions between TnC and the most C-terminal region of TnI. A deletion mutant, $TnI_{1–156}$, of chicken fast skeletal muscle TnI, equivalent to our TnI(1–159), mimicked the ability of full-length TnI to inhibit actomyosin ATPase in the absence of TnC and to release the inhibition when TnC and Ca^{2+} were added. Inhibition by full-length TnI was maintained when TnC and Mg^{2+} (but not Ca^{2+}) were added, but inhibition by $TnI_{1–156}$ was 80% reversed under these conditions (11). Thus, the C-terminal 26 residues which are missing from $TnI_{1–156}$ appear to play a role in conferring Ca^{2+} sensitivity to the regulation of muscle contraction. The structural basis for this role is not yet well understood, but a recent, detailed investigation (16) of the functional properties of a series of C-terminal deletion mutants of TnI led to the conclusion that the entire C-terminal region of TnI is needed for full regulatory activity. Ramos (16) suggested that deletion of the C-terminal 26 residues of TnI may reduce the affinity of TnI for the thin filament, thereby allowing TnC to reverse the inhibitory activity of $TnI_{1–156}$, even in the absence of Ca^{2+}.

In the present study, we have prepared a mutant, TnC*F26W*, of rabbit fast skeletal muscle TnC, which is equivalent to the spectral probe mutant of Pearlstone *et al.* (15) and contains a

[2]Abbreviations used: IAANS, 2-[4′-(iodoacetamido)anilino]-napthalene-6-sulfonic acid; IAEDANS, *N*-(iodoacetyl)-*N*′-(1-sulfo-5-naphthyl)ethylenediamine; Tn, Troponin; TnC, Troponin C; TnC*F26W*, mutant of troponin C in which Phe-26 is replaced by Trp; TnI, Troponin I; *dCW*-TnI, a Cys-less, Trp-less TnI mutant (17); TnI(1–159), deletion mutant of *dCW*-TnI containing residues 1–159; TnT, Troponin T; Tm, tropomyosin; NATA, *N*-Acetyl-L-tryptophanamide.

single Trp at position 26. We used TnC*F26W* in fluorescence lifetime and quenching studies of both isolated TnC and TnC in binary complexes with a Trp-free mutant of full-length rabbit fast skeletal muscle TnI or a truncated form of this mutant, TnI(1–159), which lacked the C-terminal 22 amino acid residues of the full-length TnI. Our results suggest for the first time that the functional importance of the C-terminal segment (residues 160–181) of TnI may be attributed, at least in part, to interactions with the regulatory, N-terminal domain of TnC.

MATERIALS AND METHODS

Protein preparation.

In these studies we used recombinant forms of TnC and TnI whose sequences were based on those of the rabbit fast skeletal muscle proteins. Our full-length TnI, *dCW*-TnI, was a Cys-less, Trp-less mutant in which the Cys-48 and Cys-64 of the wild-type protein had been replaced by Ala, Cys-133 had been replaced by Ser and Trp-160 had been replaced by Phe, prepared as described previously (17). We prepared the deletion mutant TnI(1–159) by substituting a stop codon for the Trp-160 codon in the cDNA for *dCW*-TnI. We prepared wild-type TnC as described previously (18). We prepared the single-Trp TnC mutant TnC*F26W* by substituting a Trp codon for the Phe-26 codon in the cDNA for wild-type TnC. We screened clones containing the designed mutations by DNA sequencing. For construction of TnI expression plasmids, we excised *Nco*I–*Eco*RI fragments, which contained TnI-coding sequences from double-stranded M13mp18/TnI (19) and subcloned them into *Nco*I–*Eco*RI sites of pTrc99. We expressed and purified TnC*F26W* as described by Kobayashi *et al.* (18). We expressed and purified TnI mutants as described previously (19, 20). Protein concentrations were measured by their absorbance at 280 nm. Extinction coefficients for TnC*F26W* and *dCW*-TnI were calculated using the method of Gill and von Hippel (21). Complexes of TnC*F26W* and either *dCW*-TnI or TnI(1–159) were formed by first mixing equimolar amounts of TnC and TnI in a buffer of 6 M urea, 20 mM Tris, pH 8.0, 1 M NaCl, 1 mM DTT, and 5 mM $CaCl_2$. The complexes were dialyzed against a series of buffers containing 0.1 mM DTT and decreasing concentrations of urea and NaCl and purified by ion-exchange HPLC using a Pharmacia Mono-Q column.

Fluorescence measurements.

Quantum yields and quenching of Trp fluorescence were measured on an Instruments, S.A. model Spex Fluoromax 2 fluorimeter at 25°C, with polarizers set to magic angle conditions, and an excitation wavelength of 295 nm. Quantum yields of Trp-26 in TnC*F26W* were calculated using the method of Parker and Rees (22), with Trp in water (23) as the standard. Measurements were made in a buffer solution containing 20 mM Tris, pH 8, 0.3 M KCl, and 2 mM EGTA, the same buffer plus 20 mM $MgCl_2$, and the same buffer plus 2.5 mM $CaCl_2$.

Iodide quenching was measured by titrating protein solutions with 6 M KI and observing the decrease in fluorescence intensity at the emission maximum. Samples were prepared in 20 mM Tris (pH 8.0), 2 mM EGTA, 0.1 M KCl, and 1 mM DTT. Acrylamide quenching was measured in a buffer solution containing 20 mM Tris, pH 8, 0.3 M KCl, and 2 mM EGTA, plus either 1 mM DTT (for TnC*F26W* and TnC*F26W*-TnI(1–159)) or 0.1 mM DTT (for

TnC*F26W*–*dCW*-TnI). Acrylamide quenching data was corrected for the absorbance of acrylamide at the excitation wavelength (24) and when it was nonlinear it was fit to the equation:

$$Fo/F = (1 + \mathrm{Ks}\,.\,\mathrm{v}\,.\,[Q])\mathrm{e}^{\mathrm{V}[\mathrm{Q}]}, \quad [1]$$

where *F*o and *F* are the fluorescence intensity in the absence and presence, respectively, of quencher, Ks.v. is the Stern–Volmer quenching constant, [*Q*] is the concentration of quencher, and *V* is a static quenching term. NATA, a small indole-containing molecule, was used as a standard to determine the amount of quenching expected in a fully exposed Trp side chain.

Lifetime measurements were performed using the frequency domain fluorometry technique as previously described (25–27). Excitation at 295 nm was provided by the frequency-doubled output of a rhodamine 6G dye laser synchronously pumped by a mode-locked argon ion laser. The dye laser was cavity dumped at 3.77 MHz, and measurements at higher frequencies were performed using the harmonic content of the picosecond pulses (28–30). Emission was observed at 350 nm using a 350 nm interference filter. All measurements were performed under magic angle conditions.

RESULTS

Fluorescence Properties of Isolated TnCF26W

The effects of Ca^{2+}-binding site occupancy on the steady-state fluorescence of Trp-26, the only Trp residue in TnC*F26W*, were essentially the same as those previously obtained with the equivalent TnC mutant from chicken fast skeletal muscle (15). Binding of Mg^{2+} to sites in the C-terminal domain of TnC*F26W* caused no change in quantum yield compared to the apo form, while binding of Ca^{2+} to the N-terminal domain resulted in a greater than threefold increase in quantum yield. The wavelength of the maximum fluorescence emission, λ_{max}, was essentially invariant (see Table I).

The mean fluorescence lifetime of Trp-26 increased by 15% when Mg^{2+} bound to the apo form of TnC*F26W*, and doubled when Ca^{2+} bound. The heterogeneity of the fluorescence decay increased in the Mg^{2+}-bound, but not the Ca^{2+}-bound, form, requiring a three-exponential rather than a two-exponential fit for the data. The long lifetime and high quantum yield of Trp-26 in the Ca^{2+}-bound form of TnC*F26W* indicate a significant absence of both static and solvent quenching.

A heterogeneous decay such as is seen here can be an indication of multiple species of Trp. Since our protein has a single Trp it may be an indication that the protein exists in more than one conformation simultaneously. However, this is only one of many possible causes of lifetime heterogeneity, which include protein dynamics, spectral relaxation, and other molecular interactions (24).

Fluorescence Properties of the TnC-TnI Complexes

Formation of a complex of TnC*F26W* and *dCW*-TnI had little effect on the steady-state fluorescence of Trp-26 in the absence of Ca^{2+}. The quantum yields and emission maxima of Trp-26 in both EGTA and Mg^{2+} were only slightly changed by complex formation. In the presence of Ca^{2+}, however, formation of a complex with *dCW*-TnI resulted in a 14-nm blue shift in the emission maximum and a 30% reduction in the quantum yield of Trp-26.

Formation of a complex of TnC*F26W* and TnI(1–159) in the absence of Ca^{2+} resulted in only slightly lower quantum yields of Trp-26 than those obtained from the complex with full-length *dCW*-TnI, and no difference in the emission maxima. In the presence of Ca^{2+}, however, the quantum yield of the TnC*F26W*–TnI(1–159) complex was 25% lower than the already diminished (compared to isolated TnCF26W) quantum yield of the TnC*F26W*–*dCW*-TnI complex. Both the TnC*F26W*–TnI(1–159) and TnC*F26W*–*dCW*-TnI complexes had the same blue-shifted λ_{max} of 330 nm in the presence of Ca^{2+}, indicating a substantial decrease in the exposure of Trp-26.

In the presence of EGTA, formation of the TnC–TnI complex using either *dCW*-TnI or TnI(1–159) had little effect on either the individual or the mean lifetimes of Trp-26. In the presence of Ca^{2+}, the mean lifetimes of both complexes were about 30% lower than those of isolated TnC*F26W*. A difference between the two complexes could be seen in the presence of Mg^{2+}, when the structural sites in the C-terminal domain of TnC were occupied by Mg^{2+} and the regulatory Ca^{2+}-binding sites in the N-terminal domain of TnC were vacant. Formation of the TnC*F26W*–*dCW*-TnI complex in the Mg^{2+}-bound form greatly reduced the contributions of the longest of three lifetimes, thereby lowering the mean lifetime and leaving a less heterogeneous system. When TnI(1–159) was used to form the TnC–TnI complex, the mean lifetime in the Mg^{2+}-bound form was also reduced, but the lifetime heterogeneity was more comparable to that seen in isolated TnC*F26W*.

Fluorescence Quenching by Acrylamide

Acrylamide quenching showed no significant difference in the exposure of Trp-26 between the Mg^{2+} and Ca^{2+} bound forms of isolated TnC*F26W*. Both samples showed some static quenching, as revealed by the upward curvature of the plots (Table II and Fig. 1A).

In the Ca^{2+}-bound forms, both the TnC*F26W*–*dCW*-TnI and TnC*F26W*–TnI(1–159) complexes had *k*q values that were 60% lower than the *k*q of isolated TnC*F26W* (Table II), showing a substantial reduction in the exposure of Trp-26 to acrylamide. A difference between the two complexes could be seen in their Mg^{2+}-bound forms. Under these conditions the *k*q values of isolated TnC*F26W* and the TnC*F26W*–TnI(1–159) complex were identical, but the *k*q of the TnC*F26W*–*dCW*-TnI complex was 20% lower. These results suggest that the portions of TnI, which shield Trp-26 in the Ca^{2+}-bound form are located within residues 1–159, but residues 160–181 at the C-terminus of TnI are needed for blocking access to Trp-26 in the Mg^{2+}-bound form of the TnC–TnI complex. The plots of *F*o/*F* for both complexes are linear in both the Ca^{2+}- and Mg^{2+}-bound forms, indicating an absence of static quenching (Figs. 1b and 1c).

Fluorescence Quenching by Iodide

Because of its charge and large size, iodide is considered to be a probe of surface exposure, whereas smaller, uncharged quenchers such as acrylamide can penetrate some distance into aqueous cavities below the surface and are considered to be probes of exposure to solvent. As shown by the *k*q values for iodide quenching (Table II), there was very little surface exposure of Trp-26 in any of our samples, typically about 5% that of the NATA standard in solution. For isolated TnC*F26W*, Trp-26 was about 20% less exposed to iodide in Mg^{2+} than in Ca^{2+}. Linear plots of *F*o/*F* for isolated TnC*F26W* were observed in both Mg^{2+} and Ca^{2+} (Fig. 2), indicating no charge effects. For both the TnC*F26W*–*dCW*-TnI (Fig. 3A) and TnC*F26W*–TnI(1–159) (Fig. 3B) complexes, downward curvatures of the *F*o/*F* plots in both Mg^{2+} and Ca^{2+} indicated electrostatic interactions with iodide in the vicinity of Trp-26, as demonstrated in several examples in a review by Eftink and Ghiron (31). Both TnC–TnI complexes showed a stronger downward curvature in Ca^{2+} than in Mg^{2+}, indicating a stronger electrostatic interaction with iodide in the presence of Ca^{2+}. A plausible explanation for the downward curvature is that one or more positive charges from Lys and Arg residues in the basic protein TnI raise the local concentration of the negatively charged iodide quencher near Trp-26 of TnC. Since TnI and the N-terminal domain of TnC interact more closely in Ca^{2+} than in Mg^{2+}, it is not surprising to find that the downward curvature of the *F*o/*F* plots is stronger in Ca^{2+} than in Mg^{2+}.

Downward curvature of Stern–Volmer plots may also result from the existence of multiple protein conformations, which might also cause the observed heterogeneity in the lifetimes (31). In isolated TnC*F26W*, however, the curves are linear despite lifetime heterogeneity, and no downward curvature is observed in any sample when neutral acrylamide is used as the quencher. Therefore the particular combination of a negatively charged iodide quencher and the presence of TnI must be the cause of the observed curvature, making electrostatic interaction between iodide and positive charges in the vicinity of Trp-26 the most likely cause.

In cases where downward curvature of *F*o/*F* plots were seen, the Stern–Volmer constant Ks.v. was taken to be the initial slope (31). In the Mg^{2+}-bound forms, the initial slopes suggest that there was a nearly 50% increase in iodide quenching in both complexes compared to isolated TnC*F26W*. This was much more likely due to charge effects than to any increased exposure of Trp-26. The Mg^{2+}-bound forms of our samples were also interesting in that the TnC*F26W*–TnI(1–159) complex yielded the highest *k*q value. This is reminiscent of what was seen with acrylamide quenching, where TnI(1–159) was less effective than full-length *dCW*-TnI at shielding Trp-26 from solvent effects in Mg^{2+}. The situation is different in the Ca^{2+}-bound forms, where the *k*q value for the TnC*F26W*–TnI(1–159) complex is about one sixth those of the TnC*F26W*–*dCW*-TnI complex and the isolated TnC*F26W*. It is also noteworthy that, in the Ca^{2+}-bound forms, the *k*q values for isolated TnC*F26W* and for the TnC*F26W*–*dCW*-TnI complex were nearly identical. This may be explained by competing effects which cancel each other out during the iodide quenching. A lower exposure of Trp-26 in the complex, as indicated by the acrylamide data (see above and Table I), would reduce *k*q, while introduction of an electrostatic attraction would increase *k*q. It should be noted that we were limited in the range of iodide concentration over which

data could be collected, because the exposure of Trp-26, observed as a steady growth in the amount of quenching, increased over time at ionic strengths greater than approximately 0.5.

DISCUSSION

Crystal structures of TnC with the regulatory sites filled (8) and empty (32, 33) showed that, in the Mg^{2+} bound form, the native Phe-26 side chain is only partially accessible to solvent on the outside surface of TnC. When Ca^{2+} binds to the regulatory sites in the N-terminal domain, Phe-26 is shifted so that a portion of the side chain is exposed in the middle of a newly formed hydrophobic pocket. Changes in the fluorescence properties of Trp-26 in TnC*F26W*, therefore, are good indicators for Ca^{2+}-dependent changes in the interaction of TnC and TnI. Consistent with the earlier results of Pearlstone *et al.* (15), we found that steady-state measurements of fluorescence emission maxima and quantum yields failed to show any changes in the environment of Trp-26 when Mg^{2+} bound to the C-terminal domain of the apo form of isolated TnC*F26W*. Judging by changes in the length and heterogeneity of the lifetimes, however, we found that binding of Mg^{2+} to the C-terminal sites did have some effect on the environment of Trp-26. Binding of Ca^{2+} to the N-terminal, regulatory sites of TnC*F26W* had a large effect on Trp-26 fluorescence, tripling the quantum yield and doubling the mean lifetime. Ca^{2+} binding did not change the exposure of Trp-26 to solvent, as measured by acrylamide quenching, although exposure to iodide quenching actually increased. The iodide effect may be explained by a charge-induced rearrangement of negatively charged side chains of nearby Asp and Glu residues in the vicinity of Trp-26.

In the absence of Ca^{2+} and Mg^{2+}, complex formation between TnC*F26W* and full-length *dCW*-TnI had only slight effects on the fluorescence properties of Trp-26. When the C-terminal sites of TnC*F26W* were occupied by Mg^{2+}, the effects were still quite small, observable only as shorter and less heterogeneous lifetimes than in isolated TnC*F26W*. Acrylamide quenching showed that complex formation with *dCW*-TnI partially shielded Trp-26 from solvent in the Mg^{2+} bound form, while increased exposure to iodide indicated that the basic *dCW*-TnI increased the net positive charge in the vicinity of Trp-26.

When the regulatory sites of TnC*F26W* were occupied by Ca^{2+}, complex formation with *dCW*-TnI had a pronounced effect on the fluorescence properties of Trp-26. There was a large blue shift in the emission maximum, indicating a change to a more hydrophobic environment. This is consistent with acrylamide quenching data, which showed that the exposure of Trp-26 to solvent was substantially reduced. We also observed a significantly lower quantum yield and a shorter mean lifetime upon complex formation with *dCW*-TnI. The simultaneous occurrence of all these changes is strong evidence for closer interactions between *dCW*-TnI and the N-terminal domain of TnC*F26W*.

The effects of Ca^{2+} and Mg^{2+} binding on the environment of Trp-26 in the TnC–TnI complex were different when residues 160–181 at the C-terminus of TnI were removed. Lifetime measurements in the apo and Ca^{2+}-bound forms showed no significant differences between the complexes formed using full-length *dCW*-TnI or the truncated TnI(1–159). In the Mg^{2+}-bound form, however, the Trp-26 fluorescence lifetime was more heterogeneous in

the complex formed with TnI(1–159). In this respect the TnC*F26W*–TnI(1–159) complex more closely resembled isolated TnC*F26W* than did the TnC*F26W–dCW*-TnI complex.

Acrylamide quenching and iodide quenching measurements yielded the same percentage difference in *k*q values when comparing the Mg^{2+}-bound forms of the TnC*F26W–dCW*-TnI and TnC*F26W*–TnI(1–159) complexes. This could mean that, in the Mg^{2+}-bound form, both the exposure to solvent and sensitivity to surface charge effects of Trp-26 were increased by C-terminal truncation of TnI. In the Ca^{2+}-bound form, acrylamide quenching showed that the solvent exposure of Trp-26 was not changed by C-terminal truncation of TnI, but sensitivity to surface charge effects as measured by iodide quenching was much reduced. Our results are consistent with previous studies which showed that TnI segment 115–131 binds to the N-terminal hydrophobic pocket of TnC which is exposed when Ca^{2+} binds to the regulatory sites (13, 14). Our new observations of the effects of TnI C-terminal truncation on the fluorescence properties of TnC Trp-26 indicate that a short segment at the C-terminus of TnI interacts with the N-terminal, regulatory domain of TnC in their binary complex, providing the first clue as to what role the C-terminus of TnI may play in the regulation of vertebrate striated muscle.

ACKNOWLEDGMENTS

This work was supported by NIH Grants R01-AR-41161 and T32-AR-07592 from the National Institute of Arthritis and Musculoskeletal and Skin Diseases, and by NIH Grant RR-08119 to the Center for Fluorescence Spectroscopy.

REFERENCES

1. Leavis PC, and Gergely J (1984) CRC Crit. Rev. Biochem 16, 235–305. [PubMed: 6383715]
2. Zot A, and Potter JD (1987) Annu. Rev. Biophys. Biophys. Chem 16, 535–559. [PubMed: 2954560]
3. Farah C, and Reinach FC (1995) FASEB J. 9, 755–767. [PubMed: 7601340]
4. Tobacman LS (1996) Annu. Rev. Physiol 58, 447–481. [PubMed: 8815803]
5. Squire JM, and Morris EP (1998) FASEB J. 12, 761–771. [PubMed: 9657517]
6. Herzberg O, and James MN (1985) Nature 313, 653–659. [PubMed: 3974698]
7. Sundaralingam M, Bergstrom R, Strasburg G, Rao ST, Roychowdhury P, Greaser M, and Wang BC (1985) Science 227, 945–948. [PubMed: 3969570]
8. Houdusse A, Love ML, Dominguez R, Grabarek Z, and Cohen C (1997) Structure 5, 1695–1711. [PubMed: 9438870]
9. Perry SV (1999) Mol. Cell Biochem. 190, 9–32. [PubMed: 10098965]
10. Kobayashi T, Tao T, Gergely J, and Collins JH (1994)J. Biol. Chem 269, 5725–5729. [PubMed: 8119911]
11. Farah CS, Miyamoto CA, Ramos CH, da Silva AC, Quaggio RB, Fujimori K, Smillie LB, and Reinach FC (1994) J. Biol. Chem 269, 5230–5240. [PubMed: 8106506]
12. Syska H, Wilkinson JM, Grand RJA, and Perry SV (1976) Biochem. J 153, 375–387. [PubMed: 179535]
13. McKay RT, Tripet BP, Hodges RS, and Sykes BD (1997)J. Biol. Chem 272, 28494–28500. [PubMed: 9353310]
14. Tripet B, Van Eyk J, and Hodges RS (1997) J. Mol. Biol 271, 728–750. [PubMed: 9299323]
15. Pearlstone JR, Borgford T, Chandra M, Oikawa K, Kay CM, Herzberg O, Moult J, Herklotz A, Reinach FC, and Smillie LB (1992) Biochemistry 31, 6545–6553. [PubMed: 1633166]
16. Ramos CHI (1999) J. Biol. Chem 274, 18189–18195. [PubMed: 10373418]
17. Zhao X, Kobayashi T, Malak H, Gryczynski I, Lakowicz J, Wade R, and Collins JH (1995) J. Biol. Chem 270, 15507–15514. [PubMed: 7797544]

18. Kobayashi T, Zhao X, Wade R, and Collins JH (1999) Biochim. Biophys. Acta 1430, 214–221. [PubMed: 10082949]
19. Kluwe L, Maeda K, and Maéda Y (1993) FEBS Lett. 232, 83–88.
20. Fujita S, Maeda K, and Maéda Y (1992) J. Biochem 112, 306–308. [PubMed: 1429516]
21. Gill SC, and von Hippel PH (1989) Anal. Biochem 182, 319–326. [PubMed: 2610349]
22. Parker CA, and Rees WT (1960) Analyst (London) 85, 587–600.
23. Chen RF (1967) Anal. Let 1, 35–42.
24. Lakowicz JR (1983) in Principles of Fluorescence Spectroscopy (Lakowicz JR, Ed.), pp. 258–295, Plenum Press, New York.
25. Lakowicz JR, and Maliwal BP (1985) Biophys. Chem 21, 61–78. [PubMed: 3971026]
26. Lakowicz JR, Laczko G, and Gryczynski I (1986) Rev. Sci. Instrum 57, 2499–2506.
27. Laczko G, Lakowicz JR, Gryczynski I, Gryczynski Z, and Malak H (1990) Rev. Sci. Instrum 61, 2331–2337.
28. Berndt K, Duerr H, and Palme D (1982) Opt. Commun 42, 419–422.
29. Gratton E, and Lopez-Delgado R (1980) Nuovo Cimento B56, 110–124.
30. Gratton E, James DM, Rosato N, and Weber G (1984) Rev. Sci. Instrum 55, 486–494.
31. Eftink MR, and Ghiron CA (1981) Anal. Biochem 114, 199–227. [PubMed: 7030122]
32. Herzberg O, Moult J, and James MNG (1986) J. Biol. Chem 261, 2638–2644. [PubMed: 3949740]
33. Strynadka NC, and James MN (1989) Annu. Rev. Biochem 58, 951–998. [PubMed: 2673026]

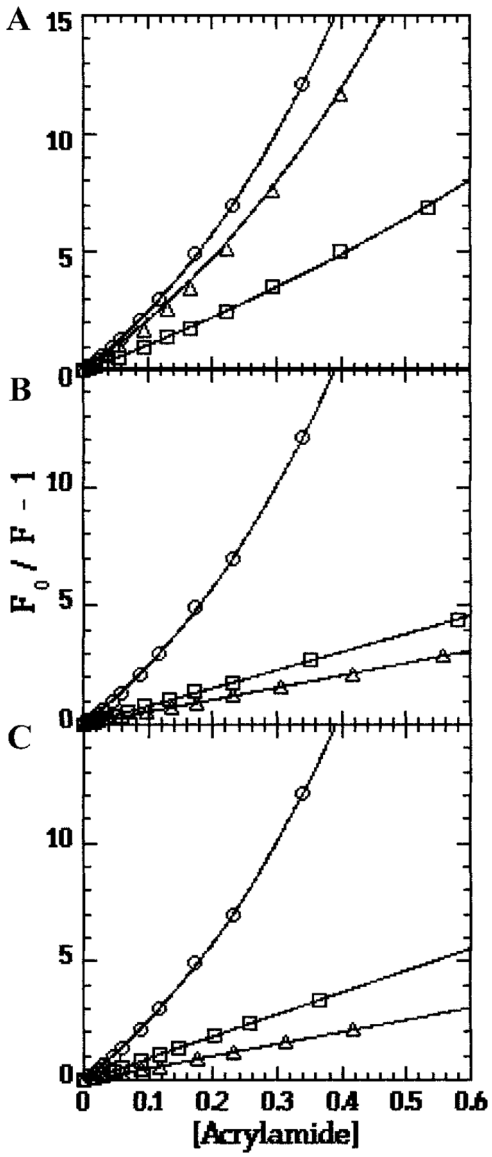

FIG. 1.

Acrylamide Quenching of Trp-26 in TnC*F26W*. (○) NATA standard, (○) Sample in Ca^{2+}, (□) Sample in Mg^{2+}. Samples: (A) isolated TnC*F26W*; (B) TnC*F26W-dCW*-TnI complex; (C) TnC*F26W*-TnI(1–159) complex.

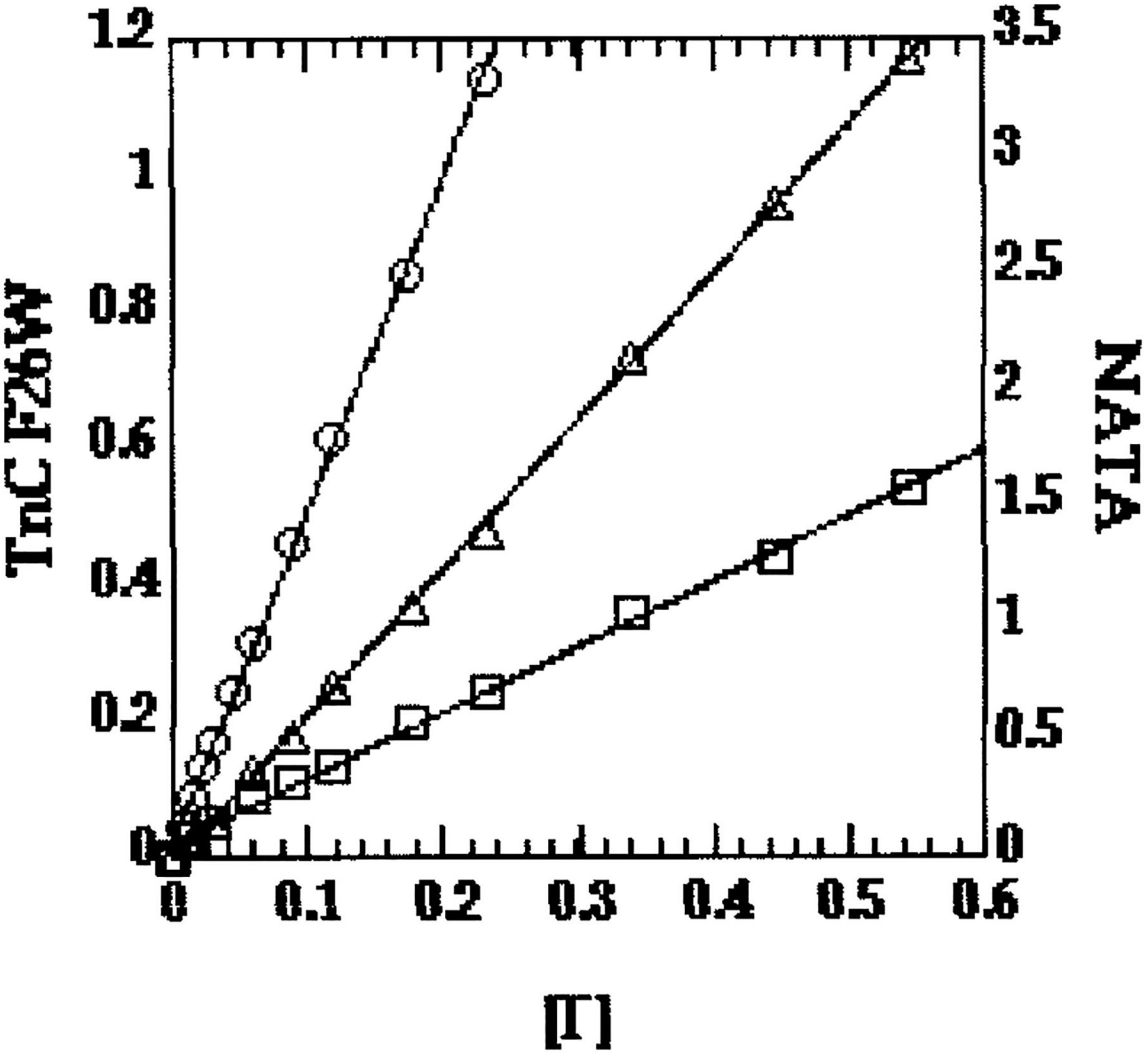

FIG. 2.

Iodide quenching of Trp-26 in isolated TnC*F26W*. (○) NATA standard, (○) Sample in Ca^{2+}, (□) Sample in Mg^{2+}.

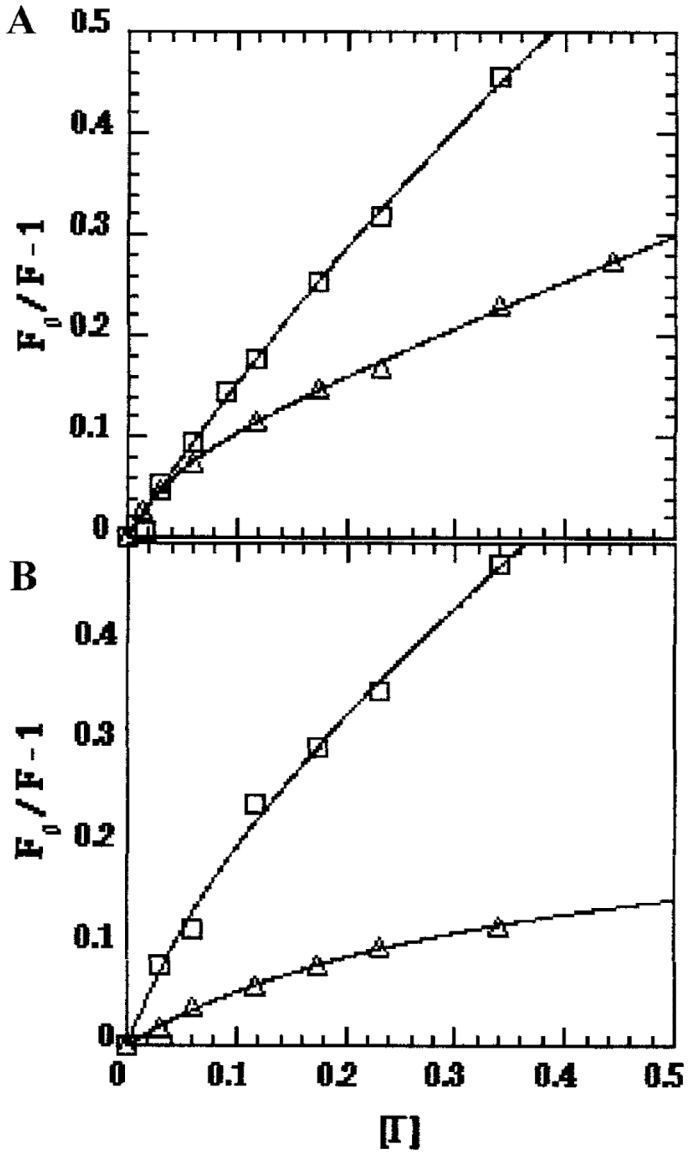

FIG. 3.

Iodide quenching of Trp-26 in TnC*F26W* when in complex with TnI. (○) Sample in Ca^{2+}, (□) Sample in Mg^{2+}. Samples: (A) TnC*F26W-dCW*-TnI complex; (B) TnC*F26W*-TnI(1–159) complex.

TABLE I

Spectral Properties of Trp-26 in TnC*F26W*

	Tn*CF26W*			Tn*CF26W-dCW*-TnI			Tn*CF26W*-TnI(1–159)		
	EGTA	**Mg^{2+}**	**Ca^{2+}**	**EGTA**	**Mg^{2+}**	**Ca^{2+}**	**EGTA**	**Mg^{2+}**	**Ca^{2+}**
λ_{max} (nm)	343	342	345	344	344	330	344	344	330
Q	0.12	0.12	0.39	0.11	0.11	0.28	0.091	0.095	0.2l
τ_{mean} (ns)	3.25	3.74	7.08	3.24	3.52	5.03	3.30	3.51	5.0l
τ1 (ns)	3.34	5.14	7.26	3.47	6.10	5.22	3.42	4.14	5.16
τ2 (ns)	0.40	2.75	1.48	0.49	3.04	0.66	0.40	2.57	0.68
τ3 (ns)		0.31			0.34			0.2l	
*A*1	0.80	0.55	0.86	0.63	0.07	0.75	0.73	0.40	0.80
*A*2	0.20	0.21	0.14	0.37	0.54	0.25	0.27	0.36	0.20
*A*3		0.24			0.38			0.24	

Note. A_i, fractional amplitude of component lifetime τ_i; *Q*, quantum yield; λ_{max}, wavelength at which maximum fluorescence emission was observed; τ_{mean}, mean lifetime.

TABLE II

Quenching of Trp-26 Fluorescence

	Tn*CF26W*		Tn*CF26W-dCW*-TnI		Tn*CF26W*-TnI(1–159)		
	Mg^{2+}	**Ca^{2+}**	**Mg^{2+}**	**Ca^{2+}**	**Mg^{2+}**	**Ca^{2+}**	**NATA**
τ_o (ns)	3.74	7.08	3.52	5.2	3.51	5.01	3.02
Ks.v. $(M^{-1})^a$	9.88	17.98	7.63	5.18	9.28	5.09	20
$V (M^{-1})^a$	0.45	1.14					1.53
$kq\ (M\ ns)^{-1}\ ^a$	2.64	2.54	2.17	1.00	2.64	1.02	6.62
kq/K^a	0.40	0.38	0.33	0.15	0.40	0.15	1.00
Ks.v. $(M^{-1})^b$	0.97	2.17	1.57	1.56	1.97	0.39	14.3
$kq\ (M\ ns)^{-1}\ ^b$	0.26	0.31	0.45	0.30	0.56	0.08	4.74
kq/K^b	0.055	0.065	0.094	0.063	0.118	0.016	1.00

Note. kq is the bimolecular quenching constant calculated from the Stern–Volmer constant Ks.v. by the equation Ks.v. = $kq^*\tau_O$; τo is the lifetime of the sample in the absence of quencher; Ks is the bimolecular quenching constant for the standard NATA.

[a] Acrylamide quenching.

[b] Iodide quenching.